Transactions, SMiRT-23
Manchester, United Kingdom - August 10-14, 2015
Division II, Paper ID 288

BIAXIAL LOADING EFFECTS ON LARGE-SCALE CRUCIFORM BENDING SPECIMENS

Caroline Meek[1], Robert Ainsworth[2]

[1]Engineering Doctorate Student, University of Manchester, Sackville Street, Manchester, UK
[2]Professor of Structural Integrity, University of Manchester, Sackville Street, Manchester, UK

ABSTRACT

To address the influence of biaxial stress effects on fracture, experimental work has been reported in the literature on cruciform specimens containing defects. For example, some large-scale tests were carried out for the US Nuclear Regulatory Commission at the Oak Ridge National Laboratory in the 1990s, concluding that biaxial loading in the form of an additional out-of-plane stress component has the effect of reducing the fracture toughness. More recently, Hohe et al. (2011) showed that these results could be reproduced using small-scale specimens. Both these studies limited the biaxial stress ratio to between 0.6 and 1.

This paper focuses on experimental data from tests on large-scale cruciform specimens carried out by the Bhabha Atomic Research Centre (BARC) in India, with biaxial stress ratios of 0, 1 and 2. The experimental results show that the biaxial loading does have an effect on the failure load. However, such biaxial effects can arise from both an influence of stress biaxiality, or constraint, on fracture toughness and an influence on crack driving force. Both these effects are discussed in this paper. The latter effect is demonstrated and reflected through an influence on the limit load when the results of the BARC tests are presented on the R6 Failure Assessment Diagram.

INTRODUCTION

There is little advice in fitness-for-service codes on dealing with the effects of biaxial loading on fracture behaviour. There has been historic research examining the effect of biaxial loading on failure parameters such as limit load and J solutions, (O'Dowd et al., 1999), (Wang, 2006), and more recent research by Lei and Budden (2014) and Meek and Ainsworth (2014) but there remains a paucity of experimental research to establish the effect of biaxial loading on fracture toughness.

Tests on plates were carried out by Wright et al., (1994) who found that a biaxial loading of approximately 0.5 times the uniaxial loading increased the fracture toughness; tests on pipes by Østby and Hellesvik (2008) found that a biaxial load increased the crack driving force. Cruciform tests enable biaxial loading to be well controlled but are rare due to the large amount of material required and expensive testing equipment. However, some large-scale tests were carried out for the US Nuclear Regulatory Commission (NRC) at the Oak Ridge National Laboratory, (McAfee, et al., 1995), (Bass et al., 1999), where it was found that biaxial loading in the form of an additional out-of-plane stress component had the effect of reducing the fracture toughness.

This paper focuses on the cruciform tests carried out more recently by the Bhabha Atomic Research Centre (BARC) in Mumbai. The results from the experimental and finite element (FE) data are compared to examine how biaxial loading influences fracture by plotting predicted failure loads on an R6 (EDF Energy Nuclear Generation Ltd, 2015) Option 1 failure assessment diagram (FAD). The influence of biaxial loading on fracture and on one aspect of the FAD, the limit load, where the effect is better

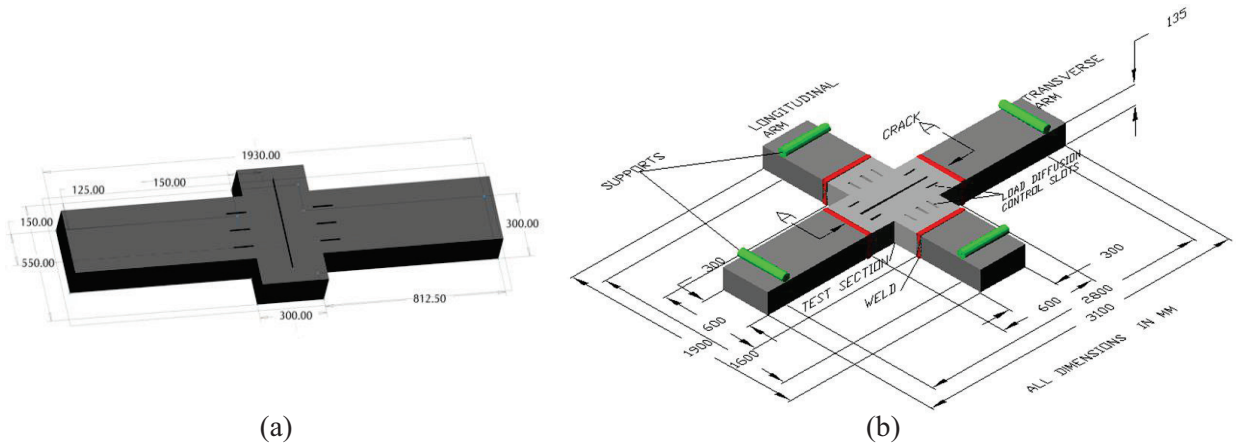

(a) (b)

Figure 1: Schematics of cruciform specimens, (a) CRRT10 and (b) CRSZ21B

understood, and recent research and results on these effects (Meek and Ainsworth, 2014), are described in the subsequent section.

EXPERIMENTAL DATA

The data analysed in this paper come from experimental and FE analysis by BARC and reported in a paper on the effect of biaxiality on fracture behaviour (Pawar et al., 2011). The tests were performed in bending on six part-through cracked 20MnMoNi55 cruciform specimens, two at room temperature (CRRT10 and CRRT11) and the remaining four at −70°C (CRSZ10, CRSZ11,CRSZ21-A and CRSZ21-B). Changing the dimensions and support locations in the cruciform specimens led to differing biaxial load ratios. Two had a biaxial load ratio B = 0, CRRT10 and CRSZ10, two were equibiaxial B = 1, CRRT11 and CRSZ11, and two had B = 2, CRSZ21-A and CRSZ21-B (see Figure 1). The normalised crack depths, a/W, were approximately 0.15 for the uniaxial specimens (B = 0) and 0.26 for the biaxial specimens (B = 1, 2).

Material properties were established using tensile tests on pipes and small-scale three point bend tests. These may be summarised as: Young's modulus E = 210 000 MPa, Poisson's ratio $\nu = 0.3$; room temperature yield strength σ_y = 490 MPa, yield strength at −70°C σ_y = 490 MPa; elastic-plastic initiation fracture toughness at room temperature J_{IC} = 250 kJ/m^2 and at −70°C, J_{IC} = 100 kJ/m^2.

Each cruciform specimen was loaded in bending to a maximum experimental load then unloaded and the extent of any crack growth from the pre-existing defect was measured. Further details of the geometry and experimental methods are given in Pawar et al (2011).

FAD INTERPRETATION OF EXPERIMENTS

Interpretation of Finite Element Analysis Results

In order to examine the effects of biaxial loading on fracture, the cruciform tests are analysed using the R6 (EDF Energy Nuclear Generation Ltd, 2015) Option 1 failure assessment diagram (FAD) (Figure 2) whose curve is given in Equation 1.

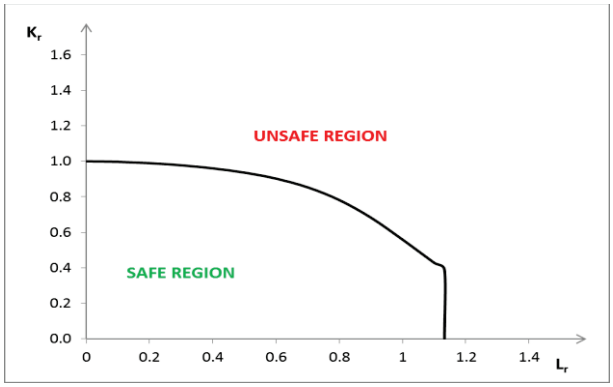

Figure 2: R6 Option 1 Failure Assessment Diagram (FAD)

$$K_r=\left[1+0.5L_r^2\right]^{-1/2}\left[0.3+0.7e^{(-0.6L_r^6)}\right] \quad (1)$$

where K_r is the proximity to linear elastic fracture, defined by

$$K_r=\frac{K}{K_{mat}}=\sqrt{\left(\frac{J_e}{J}\right)} \quad (2)$$

where K is the stress intensity factor, K_{mat} is the elastic material fracture toughness, J is the J-integral and J_e is the elastic component of the J-integral; and L_r is the proximity to plastic collapse defined by

$$L_r=\frac{F}{F_0} \quad (3)$$

where F is the applied load and F_0 is a reference or limit load.

In the absence of stress intensity factor and limit load solutions, a method proposed by Zerbst et al. (2012) has been adapted in order to provide these inputs from FE analyses given in Pawar et al (2011) and hence enable failure assessment diagram assessments of failure load to be made.

First, the figures of J versus load in Pawar et al (2011) have been digitised. The elastic J_e has then been found by fitting a quadratic function, J_e = constant * load^2, to the lower load part of the graph. This then defines the stress intensity factor for each specimen. It was found that the solutions were very close to those obtained from application of the equations of Hohe et al. (2011), although the geometries considered here are strictly outside the range of application of these equations.

Having deduced J_e, values of J/J_e were obtained from the J-integral versus load curves for the FE models of the six cruciform specimens given in Pawar et al. (2011). The method of Zerbst et al. (2012) proposes that since the reference load F_0 is the load for which $L_r = 1$, i.e., from Equation 1, the load for which $K_r = 0.559$, it is the load for which $J/J_e = 3.2$ (Equation 2). However, the values of J/J_e found from the FE analyses in Pawar et al. (2011) do not exceed 3.05 and thus it is not possible to apply the method of

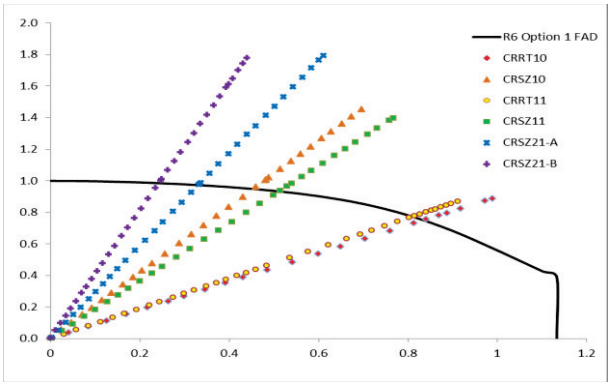

Figure 3: R6 Option 1 FAD, all specimens

Zerbst et al. (2012) directly. Instead, the reference load F_0 is found by calculating, for the maximum FE load for each specimen, the value of K_r from Equation 2 using the calculated value of J/J_e and hence the corresponding value of L_r using Equation 1. The maximum FE load is then divided by this value of L_r to give the load for which $L_r = 1$, i.e. the limit load or reference load, F_0, for each specimen; these are listed in Table 1.

It should be recognised that the limit load F_0 obtained by this method is subject to some uncertainty when the value of K_r is close to unity, since Equation 1 is then only weakly dependent on L_r. This is why Zerbst et al. (2012) proposed to use a high value of J/J_e, i.e. a lower value of K_r. Although, in the absence of results at higher J/J_e it has not been possible to apply the method of Zerbst et al. (2012) directly, it is noted that at low K_r the FAD assessments of the tests are not sensitive to the deduced values of F_0. Therefore, in particular, although the estimate of F_0 for test CRSZ21-B appears high, this has little influence on the corresponding estimate of initiation load.

FAD assessments for the different values of B have then been performed by plotting the K_r vs L_r locus for each specimen on an R6 Option 1 FAD (Figure 3) using the initiation fracture toughness values given above. The predicted initiation loads, i.e. the loads at which the plotted K_r vs L_r loci meet the R6 Option 1 FAD, are plotted against biaxial ratio B in Figure 4. These results are discussed below and compared to the experimental data.

Table 1: Results of FE analysis on cruciform specimens

Specimen	Max FE Load (kN)	J/J_e at Max FE Load	K_r at Max FE Load	L_r at Max FE Load	Reference Load, F_0 (kN)
CRRT10	2560	3.05	0.572	0.99	2586
CRSZ10	2493	1.37	0.856	0.70	3575
CRRT11	3576	2.23	0.670	0.91	3926
CRSZ11	3801	1.53	0.808	0.77	4955
CRSZ21-A	3011	1.24	0.898	0.61	4927
CRSZ21-B	3099	1.10	0.952	0.44	7016

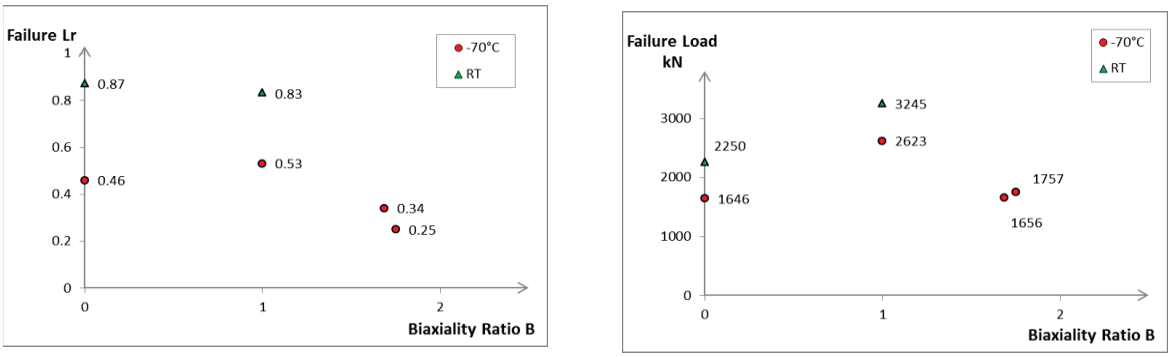

(a) (b)

Figure 4: Failure load vs biaxial ratio

Experimental Results

The experimental results of the tests on cruciform specimens are presented in Table 2 and compared to the predicted initiation loads using the FAD approach above, and also the predicted initiation loads obtained by Pawar et al. (2011) as the loads for which the FE values of J were equal to the initiation fracture toughness. The two prediction approaches are similar, not surprisingly since the FAD inputs have been based on the FE data.

For the uniaxial specimens, the initiation loads predicted by the FAD assessments in Table 2 are below the experimentally applied loads and hence some crack growth would be predicted in the experiments. The observed crack growth is however small and so the FAD assessments appear to be conservative. The equibiaxial specimens did not show any crack growth, even though for the low temperature specimen the test maximum load 3007 kN exceeds that predicted for initiation by the FAD assessment using uniaxial bend specimen fracture toughness. It can be seen from the Table 2 that the values of crack growth for the two biaxial specimens with B = 2 differ significantly, although they are almost identical in geometry and loading. The applied loads are well in excess of the predicted initiation loads suggesting that the FAD and FE assessments are overly conservative in this case.

Table 2: Results of experiments on cruciform specimens

Specimen	Max Load (kN)	Maximum Crack Growth (mm)	FE Predicted Crack Growth Initiation Load (kN)	FAD Predicted Crack Growth Initiation Load (kN)
CRRT10	2715	0.7	2300	2250
CRSZ10	2730	0.1	1730	1646
CRRT11	3037	0.0	3380	3245
CRSZ11	3007	0.0	2675	2623
CRSZ21-A	2766	1.2	1638	1656
CRSZ21-B	2805	0.2	1742	1757

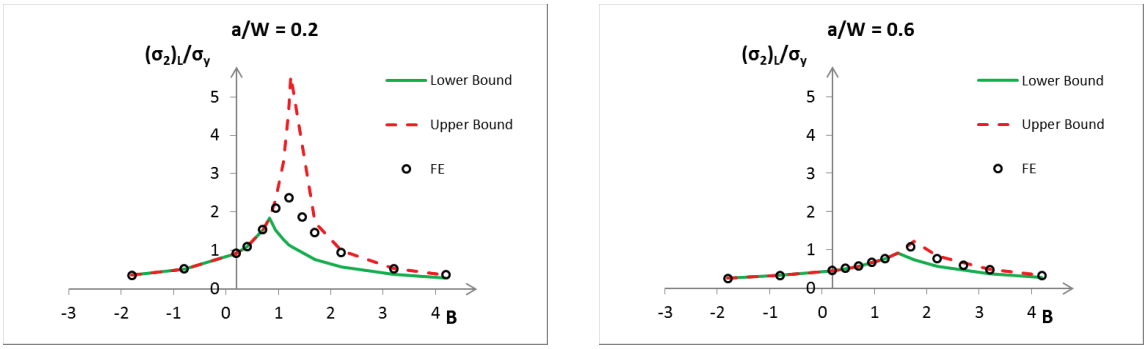

(a) (b)

Figure 5: Limit loads for centre cracked plates, H/W = 2

GENERAL EFFECTS OF BIAXIALITY ON FAD ASSESSMENT

It can be seen from both the experimental loads in Table 2 and the predicted initiation loads in Figure 4(b), that there is not a monotonic effect of biaxiality on fracture load. The fracture loads for B = 0 and B = 2 are similar, while those for B = 1 are higher. These effects are discussed in this section in terms of the general effects of biaxiality on fracture.

Theoretical and numerical FE analyses have been used by the authors to determine the effect of biaxial loading on the limit load for a number of plate geometries in plane strain and the trends with biaxiality are exemplified by those for centre cracked plates (Meek and Ainsworth, 2014). For a range of crack sizes, upper and lower bound limit loads. as well as estimates from FE analysis, have been determined and these show (see Figure 5) that as the biaxial ratio increases, the limit load increases until the biaxial load ratio B reaches approximately 1 (equibiaxial loading); thereafter the limit load decreases.

The non-monotonic trends in Figure 5 are consistent with those in Figure 4(b). In general, negative and high positive values of B lead to a reduction in the limit load relative to that for uniaxial loading (B = 0), whereas loadings close to equibiaxiality (B = 1) lead to increases in the limit load. Thus, negative and high positive values of B lead to increased plasticity and hence increased crack driving force for a given load normal to the defect, relative to the uniaxial case, whereas B = 1 leads to a reduced crack driving force. Therefore, the non-monotonic variations with B for the experimental and predicted initiation loads for the cruciform specimens are consistent with the general trends of crack driving force with biaxiality.

For predicting fracture behaviour, however, not only the crack driving force but also the material resistance to fracture is important. Thus, the behaviour described above is complicated by the influence of biaxiality on fracture toughness.

In R6 (EDF Energy Nuclear Generation Ltd, 2015), the constraint dependent fracture toughness, K^c_{mat}, is related to the high constraint fracture toughness, K_{mat}, by

$$K^c_{mat} = K_{mat}[1+\propto(-\beta L_r)^m] \quad (4)$$

where β is a normalised measure of constraint discussed below and α, m are material and temperature dependent constants with $\alpha = 0$ for high constraint, $\beta \geq 0$. In the ductile regime, α and m are, additionally, functions of ductile crack growth. Forms other than Equation 4 have been used in the

literature but the discussion of this section is not affected by any particular relationship between K^c_{mat} and K_{mat}.

The constraint parameter β is here considered to be defined by the elastic T-stress as

$$\beta = \frac{T}{L_r \sigma_y} \tag{5}$$

A number of observations may be made:

A. Firstly, the behaviour depends on material and fracture mode. For cleavage fracture and toughness after significant ductile crack growth, there can be a significant elevation in K^c_{mat} above K_{mat}, whereas for ductile initiation the effects tend to be rather smaller.
B. Secondly, the constraint effect depends on the extent of plasticity, as represented by the value of L_r in Equation 4. Thus, at low L_r, constraint effects are smaller whereas at high L_r they can be much greater.
C. Thirdly, the constraint effects depend on the magnitude of the T-stress, which is proportional to load so that β is independent of load. For deeply cracked bend specimens used for fracture toughness testing, constraint is high ($\beta > 0$), whereas for shallow cracks in uniaxial tension, constraint can be low ($T < 0$). Positive biaxial loads increase the T-stress whereas negative B reduces T.

For the cruciform tests at low temperature, the fracture toughness is relatively low and fracture initiation occurs at low values of L_r (< 0.77). Therefore, in view of (A) and (B), constraint effects would not be expected to be large and the effects of biaxial loading would be expected to be dominated by the effects on crack driving force via the effects on F_0. The maximum experimental loads for B = 0 and B = 2 are within 3% of each other whereas for B = 1, the loads are 10% higher. While this is consistent with the trends in Figure 5, it should be recognised that for a given load, the stress intensity factor in the cruciform specimen with B = 2 is higher than for the uniaxial case and this leads to a reduction in predicted initiation load, below that observed experimentally.

For the two cruciform tests at room temperature, a significant effect of biaxiality on limit load and predicted initiation load is predicted (45%), without any effect of constraint. The observed increase (12%) in maximum experimental load is rather smaller but no ductile crack growth was observed in the specimen with B = 1. Therefore, the results are not inconsistent with the predictions or with generally expected trends.

CONCLUSIONS

1. A method proposed by Zerbst et al. (2012) has been adapted to estimate the limit load for cruciform bend specimens from finite element J solutions.
2. The estimates of limit load have been used to perform FAD assessments of 6 cruciform bend specimens with a range of biaxial load ratios. The assessments lead to predictions of initiation load which are similar for B = 0 and B = 2 but higher for B = 1, broadly in line with the experimental results.
3. The predictions above are consistent with the effects of biaxiality on limit load deduced from the finite element J solutions and with generally expected trends. Thus, the influence of biaxiality in

these tests appears to be dominated by the effects on crack driving force, through the effect on limit load, rather than as a result of constraint effects on fracture toughness.

ACKNOWLEDGEMENTS

The authors wish to acknowledge support (including an EngD studentship) from the Engineering and Physical Sciences Research Council, EDF Energy and AMEC Foster Wheeler.

NOMENCLATURE

a	Crack size in cruciform specimen, half crack size in centre cracked plate
B	Biaxial load ratio
E	Young's modulus
F	Load applied during cruciform testing
F_0	Reference load
H	Half plate height
J	J-integral, elastic-plastic crack tip characterizing parameter
J_e	Elastic component of J-integral
J_{IC}	Elastic-plastic fracture toughness
K	Stress intensity factor
K_{mat}	Material fracture toughness
K_{mat}^c	Constraint dependent fracture toughness
K_r	Proximity to LEFM failure = K/K_{mat}
L_r	Proximity to plastic collapse
m	Constant describing influence of constraint on fracture toughness
T	Elastic T-stress
W	Width in cruciform specimen, half plate width in centre cracked plate
α	Constant describing influence of constraint on fracture toughness
β	Normalised constraint parameter
σ_y	Yield stress

REFERENCES

Bass, B.R., McAfee, W.J., Williams, P.T. and Pennell, W.E. (1999), "Fracture assessment of shallow-flaw cruciform beams tested under uniaxial and biaxial loading conditions", *Nuclear Engineering and Design*, Vol. 188 No. 1999, pp. 259–288.

EDF Energy Nuclear Generation Ltd. (2015), *R6: Assessment of the Integrity of Structures Containing Defects*, EDF Energy Nuclear Generation Ltd, Gloucester, UK, Revision 4.

Hohe, J., Luckow, S., Hardenacke, V., Sguaizer, Y. and Siegele, D. (2011), "Enhanced fracture assessment under biaxial external loads using small scale cruciform bending specimens", *Engineering Fracture Mechanics*, Vol. 78 No. 9, pp. 1876–1894.

Lei, Y. and Budden, P.J. (2014), "Limit load solutions of plates with extended surface cracks under combined biaxial forces and cross-thickness bending", *The Journal of Strain Analysis for Engineering Design*, Vol. 49, pp. 533–546.

McAfee, W.J., Bass, B.R., Bryson Jr., J.W. and Pennell, W.E. (1995), *Biaxial Loading Effects on Fracture Toughness of Reactor Pressure Vessels*, USNRC Report NUREG/CR-6273, Oak Ridge National Laboratory, Tennessee, USA.

Meek, C. and Ainsworth, R.A. (2014), "Fracture assessment of centre-cracked plates under biaxial loading", *Procedia Materials Science*, Vol. 3, pp. 1612–1617.

O'Dowd, N.P., Kolednik, O. and Naumenko, V. (1999), "Elastic-plastic analysis of biaxially loaded center-cracked plates", *International Journal of Solids and Structures*, Vol. 36, pp. 5639–5661.

Østby, E. and Hellesvik, A.O. (2008), "Large-scale experimental investigation of the effect of biaxial loading on the deformation capacity of pipes with defects", *International Journal of Pressure Vessels and Piping*, Vol. 85 No. 11, pp. 814–824.

Pawar, A.K., Sahu, M.K., Chattopadhyay, J., Dutta, B.K., Vaze, K.K., Gandhi, P. and Raghava, G. (2011), "Effect of biaxiality on fracture behavior : testing and analysis of cruciform specimen", *SMiRT 21, 6-11 November*, New Delhi, Vol. 1, pp. 6–11.

Wang, X. (2006), "Fully plastic J-integral solutions for surface cracked plates under biaxial loading", *Engineering Fracture Mechanics*, Vol. 73 No. 11, pp. 1581–1595.

Wright, D.J., Sharples, J.K., Sherry, A.H. and Gardner, L. (1994), "Effect of biaxial loading on the fracture behaviour of a ferritic steel component", *Nuclear Engineering and Design*, Vol. 152, pp. 39–55.

Zerbst, U., Ainsworth, R. A. and Madia, M. (2012), "Reference load versus limit load in engineering flaw assessment: A proposal for a hybrid analysis option", *Engineering Fracture Mechanics*, Vol. 91, pp. 62–72.